### **CLIMATE CHANGE**

# Chemistry-albedo feedbacks offset up to a third of forestation's CO<sub>2</sub> removal benefits

James Weber<sup>1\*</sup>, James A. King<sup>1</sup>, Nathan Luke Abraham<sup>2,3</sup>, Daniel P. Grosvenor<sup>4,5</sup>, Christopher J. Smith<sup>6,7</sup>, Youngsub Matthew Shin<sup>2</sup>, Peter Lawrence<sup>8</sup>, Stephanie Roe<sup>9</sup>, David J. Beerling<sup>1</sup>, Maria Val Martin<sup>1\*</sup>

Forestation is widely proposed for carbon dioxide (CO<sub>2</sub>) removal, but its impact on climate through changes to atmospheric composition and surface albedo remains relatively unexplored. We assessed these responses using two Earth system models by comparing a scenario with extensive global forest expansion in suitable regions to other plausible futures. We found that forestation increased aerosol scattering and the greenhouse gases methane and ozone following increased biogenic organic emissions. Additionally, forestation decreased surface albedo, which yielded a positive radiative forcing (i.e., warming). This offset up to a third of the negative forcing from the additional CO<sub>2</sub> removal under a 4°C warming scenario. However, when forestation was pursued alongside other strategies that achieve the 2°C Paris Agreement target, the offsetting positive forcing was smaller, highlighting the urgency for simultaneous emission reductions.

eforestation and afforestation are widely proposed nature-based strategies for atmospheric carbon dioxide (CO2) removal (CDR) and climate change mitigation (1). These strategies have the potential to provide additional benefits for biodiversity; multiple ecosystem services, including reduced soil erosion and climate resilience; and forestry products and local cooling through transpiration (2-4). The Bonn Challenge, the New York Declaration on Forests, and the UN Decade on Ecosystem Restoration set a target to restore 350 Mha of degraded and deforested lands by 2030 (5). However, wide-scale forest expansion drives biophysical feedbacks within the Earth system that may lead to warming. For example, darker forests decrease surface albedo, which can substantially offset the cooling effects of carbon sequestration in some regions of the world (6, 7).

Forests also release substantial quantities (760 TgC yr<sup>-1</sup>) of biogenic volatile organic compounds (BVOCs) that affect the greenhouse gases ozone ( $O_3$ ) and methane (CH<sub>4</sub>), as well as organic aerosols, with complex impacts on climate (8, 9). Chemical reactions of BVOCs deplete the hydroxyl radical (OH), increasing

<sup>1</sup>Leverhulme Centre for Climate Change Mitigation, School of Biosciences, University of Sheffield, Sheffield S10 2TN, UK. <sup>2</sup>Centre for Atmospheric Science, Yusuf Hamied Department of Chemistry, University of Cambridge, Cambridge CB2 1EW, UK. <sup>3</sup>National Centre for Atmospheric Science, Yusuf Hamied Department of Chemistry, University of Cambridge, Cambridge CB2 1EW, UK. 4Centre for Environmental Modelling and Computation (CEMAC), School of Earth and Environment, University of Leeds, Leeds LS2 9JT, UK. 5Met Office Hadley Centre, Exeter EX1 3PB, UK. 6Institute for Climate and Atmospheric Science, School of Earth and Environment, University of Leeds, Leeds LS2 9JT, UK, International Institute for Applied Systems Analysis, A-2361 Laxenburg, Austria. 8NCAR Earth System Laboratory, Climate and Global Dynamics Division, National Center for Atmospheric Research, Boulder, CO 80307, USA. 9World Wildlife Fund, Washington, DC 20037, USA.

\*Corresponding author. Email: j.m.weber@reading.ac.uk (J.W.); m.valmartin@sheffield.ac.uk (M.V.M.)

 ${\rm CH_4}$ ; drive  ${\rm O_3}$  production or loss depending on the chemical environment; and produce oxidation products, which can add to or form aerosols that interact with solar radiation. Changes to atmospheric composition have been shown to be important in the net climatic impact of instantaneous global deforestation (10), and that which occurred between years 1850 and 2000 from cropland expansion (11). However, the atmospheric composition's response to proposed reforestation and afforestation programs under different 21st-century future climate pathways, as well as their effects on climate, have received less consideration.

We present an assessment of climate feedbacks from a large-scale afforestation, reforestation, and forest enhancement (hereafter, all three are referred to as "forestation") scenario. To

mitigate possible single-model bias (8), we formed the same experiments in two stat the-art climate models, UKESM1 (12) and CESM2 (13), which feature interactive atmospheric chemistry, aerosols, and BVOC emission schemes. We used a land surface cover scenario, which we named Maxforest, that expands forests from 2015 land cover in biomes where trees are expected to thrive: through reforestation (of rangeland, secondary forest, and secondary nonforest in forest biomes), forest enhancement (of forests where tree cover density is less than its potential), and afforestation (of rangeland, secondary forest, and secondary nonforest in nonforest biomes where tree cover is >10%) (14). The Maxforest scenario represents a nearbiophysical maximum for forestation given constraints on the rate of forestation and excluding expansion on croplands, pasturelands, urban lands, and protected areas designated by the International Union for Conservation of Nature (supplementary materials, Maxforest Scenario). This scenario resulted in additional tree cover of 500 Mha by 2050 rising to 750 Mha in 2095 (relative to 2015) (Fig. 1A), with approximately 55% from afforestation, 25% from reforestation, and 20% from forest enhancement by 2095. Although large-scale forestation presents certain risks and trade-offs (1), we used this theoretical biophysical maximum forestation scenario for

We compared Maxforest to two well-established future scenarios: SSP3-7.0 (regional rivalry), which features resource-intensive consumption, diminished technology development, and very low climate change mitigation efforts leading to global warming up to 4°C above preindustrial temperatures; and SSP1-2.6 (sustainability), which is characterized by inclusive development, environmental management, and lower

our assessment to best detect biophysical changes.

Table 1. Modeling experiments in UKESM1 and CESM2.

Simulations <sup>a</sup>	Land surface cover (forest cover change at 2095 relative to 2015)	Simulation conditions <sup>b</sup>	ΔGlobal tree cover (MF – SSP) at 2050 (2095)	$\Delta BVOC$ emissions (MF - SSP) at 2050 (2095) <sup>c</sup>
4C_SSP3	SSP3	SSP3-7.0	15%	17 to 19%
	(deforestation,	(High warming up	(26%)	(32 to 38%)
	-290 Mha)	to 4°C, small		
4C_MF	Maxforest	air pollution decrease)		
	(extensive forestation,			
	+750 Mha)			
2C_SSP1	SSP1	SSP1-2.6	6%	8%
	(forestation, +300 Mha)	(Low warming up	(10%)	(11 to 13%)
2C_MF	Maxforest	to 2°C, large		
	(extensive forestation, +750 Mha)	air pollution decrease)		
<sup>a</sup> Simulations performed at years 2050 and 2095. <sup>b</sup> Well-mixed greenhouse gases, anthropogenic and biomass-burning				

<sup>a</sup>Simulations performed at years 2050 and 2095. <sup>b</sup>Well-mixed greenhouse gases, anthropogenic and biomass-burnin emissions, and sea-surface temperatures. <sup>c</sup>Range shows model variation.

resource- and energy-intensive consumption with much stronger efforts to mitigate climate change, limiting warming to  $<2^{\circ}$ C (I5). The land surface cover projection of SSP3-7.0 includes high levels of deforestation relative to that of 2015 (-290 Mha by 2095), whereas SSP1-2.6 has forestation that, at 310 Mha by 2095, is already 40% of the increase in Maxforest (Fig. 1). The extensive mitigation efforts in SSP1-2.6 also lead to lower well-mixed greenhouse gas concentrations ( $CO_2$ ,  $CH_4$ , and nitrous oxide) than that of SSP3-7.0 and greater reductions to anthropogenic emissions of other climatically relevant air pollutants, such as nitrogen oxides ( $NO_x$ ) (figs. S2 and S3 and table S1).

Specifically, we compared contemporaneous pairs of model simulations at years 2050 and 2095: a control run with land cover and atmospheric conditions from SSP3-7.0 or SSP1-2.6 (referred to as 4C\_SSP3 and 2C\_SSP1, respectively) and a run identical except for the substitution of land cover from Maxforest (4C MF and 2C MF) (Table 1). These simulations used prescribed sea-surface temperatures and sea ice. The land surface cover, described in terms of the fraction of each land surface type (trees, grassland, crops, urban, etc.) in each model grid cell, was fixed to scenario-specific values (Table 1). Thus, no deviation from the scenarios occurred over the course of the model simulations. This approach allowed the effective radiative forcing to be calculated (16). However, the emissions of BVOCs from vegetation into the atmosphere were still interactively simulated based on the vegetation type by using the standard MEGAN (CESM2) (17) and iBVOC (UKESM1) (18) schemes, linking forestation to atmospheric composition. Thus, we isolated the effects of forestation on surface albedo and atmospheric chemical composition under two possible futures. We calculated the resulting change in the atmosphere's energy balance [the radiative forcing (RF)] in 4C\_MF and 2C\_MF relative to that of the corresponding control simulation (4C\_SSP3 and 2C\_SSP1), with a focus on changes to surface albedo (RF<sub>Alb</sub>), aerosol scattering (RFAer), CH4 (RFCH4), and  $O_3$  (RF<sub>O3</sub>). We compared this to the climatic impact of the extra CDR from Maxforest's additional forestation, calculated with CLM5, the CESM2 land surface component (table S2), as Maxforest was originally developed within CESM2 to establish the net climate benefit.

To isolate the effect of BVOC changes while ensuring comparability with the SSP pathways, we kept the fire- and ozone-induced damage modules inactive in both UKESM1 and CESM2, i.e., we did not consider how fire emissions would respond to forestation or the effect of surface ozone damage on forest carbon uptake (19, 20). For fire emissions, we used the same prescribed biomass burning emissions for simulation pairs. For example, both 4C\_SSP3 and 4C\_MF scenarios used biomass burning

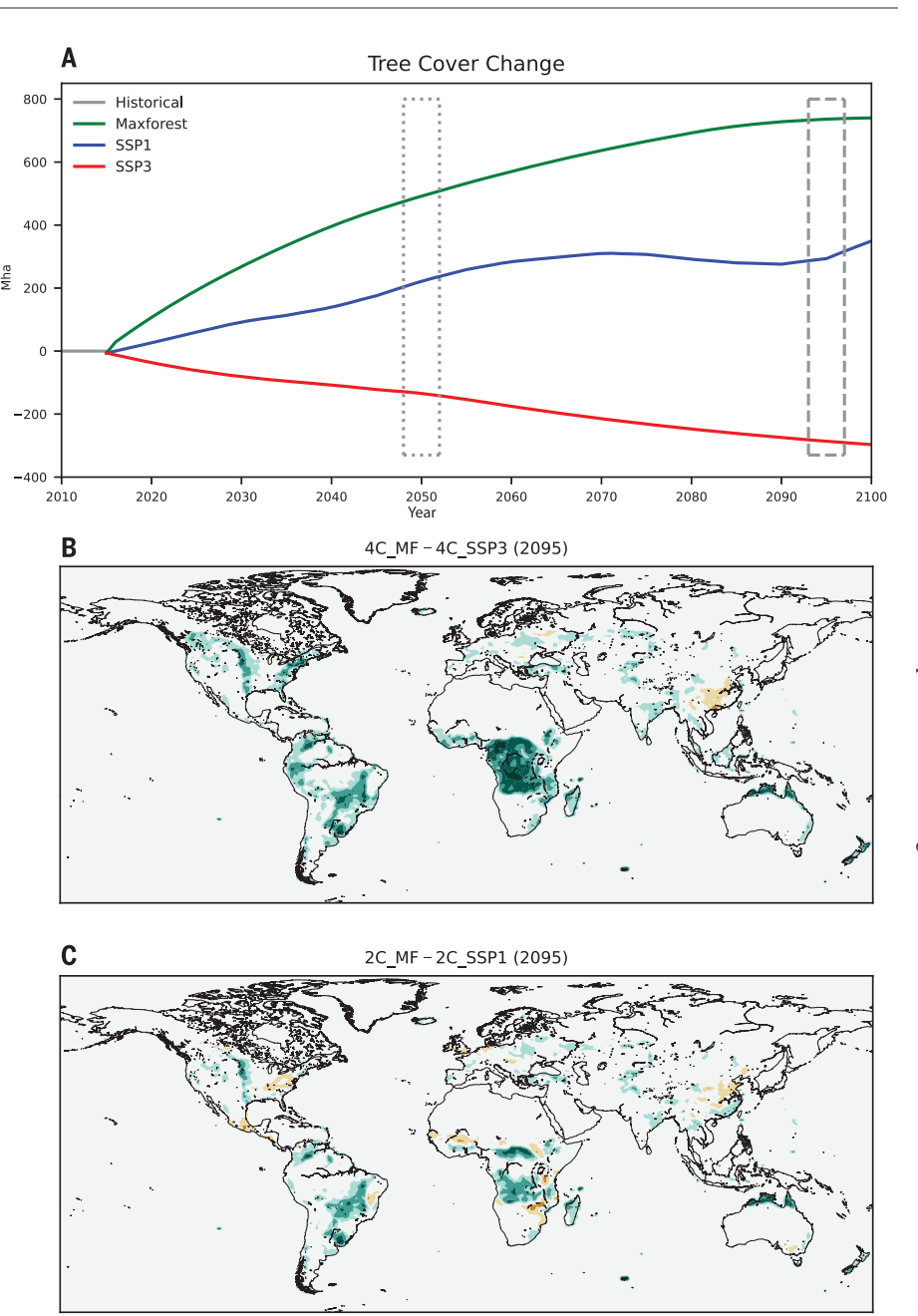


**Fig. 1. Tree cover change.** (**A**) Total change in tree cover relative to the historical 2010 to 2014 mean for the Maxforest (MF), SSP3, and SSP1 land surface cover scenarios. The dotted and dashed boxes indicate time periods considered in this study (2050 and 2095, respectively). Also shown are the percentage differences in tree cover at 2095 between (**B**) 4C\_MF and 4C\_SSP3 and (**C**) 2C\_MF and 2C\_SSP1, corresponding to dashed region in (A).

emissions from SSP3-7.0 in 2050 and 2095 (supplementary materials, Earth Systems Model Simulations).

By embedding Maxforest's land surface cover into simulations that used SSP3-7.0 and SSP1-2.6 atmospheric conditions, we provide thorough insights into forestation's impacts on atmospheric composition and climate in two contrasting futures. Our comprehensive analysis extends earlier work that considered the climatic impact of extensive forestation from CDR (21) or, in some cases, albedo changes as well (7).

## Results

We found that the global net RF (RF  $_{net}$  = RF  $_{Alb}$  + RF  $_{Aer}$  + RF  $_{CH4}$  + RF  $_{O3}$  ) from changes to

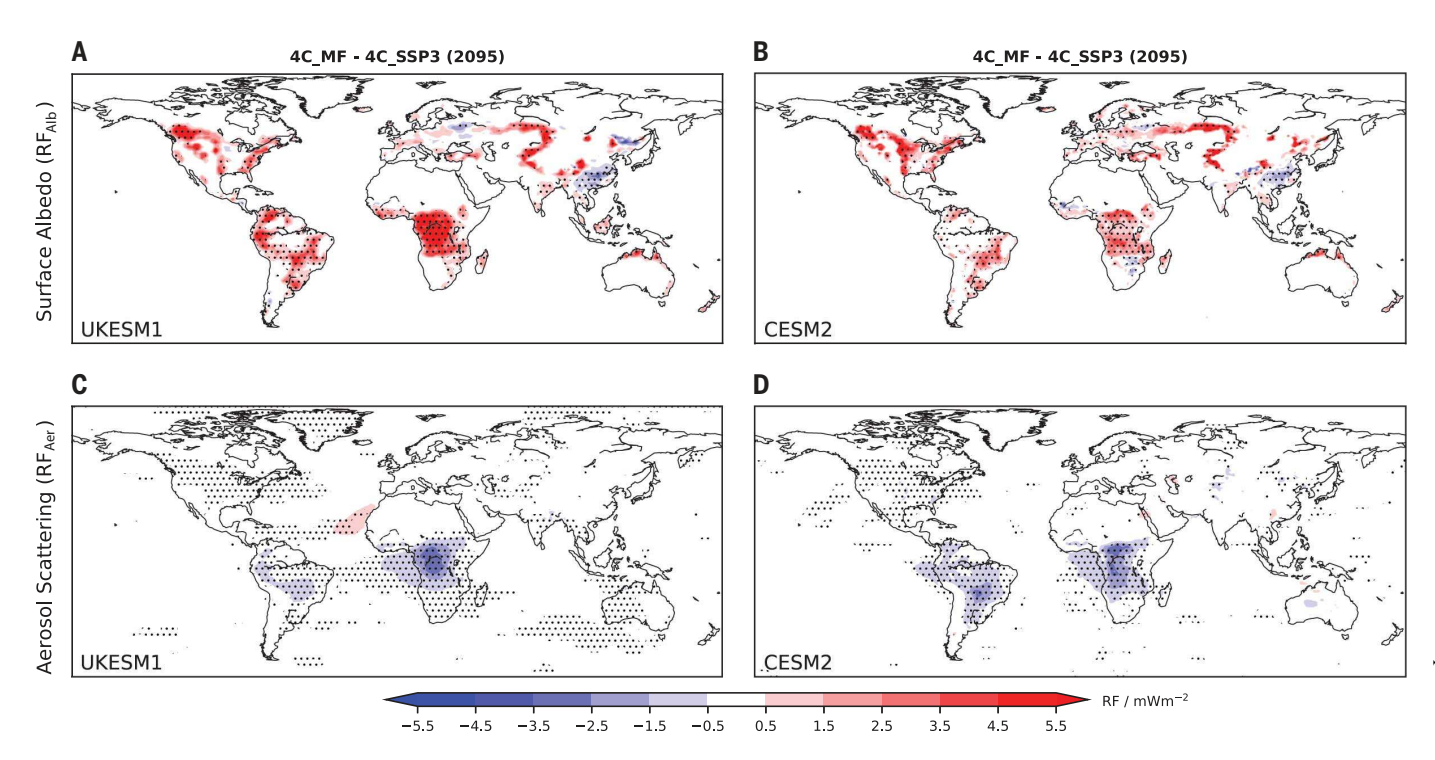


Fig. 2. Surface albedo and aerosol scattering. RF<sub>Alb</sub> and RF<sub>Aer</sub> between 4C\_MF and 4C\_SSP3 in (**A** and **C**) UKESM1 and (**B** and **D**) CESM2 at 2095. Stippling shows regions of statistical significance at 95% confidence.

surface albedo, aerosol scattering, CH<sub>4</sub>, and O<sub>3</sub> from forestation was, in all cases, positive (i.e., corresponding to a warming) and relatively consistent between the models. Compared with 4C\_SSP3, RF<sub>net</sub> in 4C\_MF was 90 to 104 mW m<sup>-2</sup> (range here and throughout indicates the two-model range unless otherwise stated) at 2050, rising to 101 to 192 mW m<sup>-2</sup> at 2095. This is equivalent to CO2 increases of 9 to 11 ppm (2050) and 16 to 30 ppm (2095) (supplementary materials, Radiative Forcing Calculations). The smaller increase in tree cover and BVOC emissions in 2C\_MF relative to 2C\_ SSP1 led to a smaller  $RF_{net}$  of 8 to 56 mW  $m^{-2}$ at 2050 and 41 to 63 mW m<sup>-2</sup> at 2095, which are equivalent to CO<sub>2</sub> increases of 1 to 5 ppm (2050) and 5 to 10 ppm (2095).

## Surface albedo and aerosol scattering

We first assessed the extent to which reductions in surface albedo arising from the expansion of forests (22) were offset by enhanced aerosol scattering following increases in organic aerosol produced from BVOC oxidation.

In the tropics, forest expansion led to both models simulating positive RF<sub>Alb</sub>, although the magnitude in UKESM1 was about twice that of CESM2 (Fig. 2, A and B, and fig. S6). The increase in BVOC emissions and subsequent organic aerosol from BVOC oxidation products (fig. S4 and S5) yielded a negative forcing from aerosol scattering (RF<sub>Aer</sub>) (Fig. 2C and fig. S6), which offset some of the positive RF<sub>Alb</sub>. The spatial distribution of RF<sub>Aer</sub> correlated

well with the regions exhibiting the greatest increases in organic aerosol. In 2095, under 4C and 2C conditions, aerosol scattering offset about 50% of  $RF_{Alb}$  in UKESM1 and the entirety in CESM2 (Fig. 3, C and D).

At higher latitudes, the effect of forestation on surface albedo was more pronounced than in the tropics owing to the lower albedo of the forest and seasonal snow cover (which greatly increases albedo for periods of the year when snow can settle on nonforested land). As a result, the reduction in albedo per unit area of forestation was much higher than in the tropics. Furthermore, lower temperatures at higher latitudes limited the BVOC emissions (Fig. 3B), resulting in reduced organic aerosol production and a smaller RF $_{\rm Aep}$  meaning that at higher latitudes, the warming from surface albedo changes tended to outweigh the cooling from aerosol scattering (Fig. 3C).

The greater RF<sub>Alb</sub> per unit area of forestation at high latitude supports previous findings that high latitude forestation is likely to produce net warming owing to albedo decreases (22). However, we extended this by illustrating how the cooling effect of aerosol scattering, particularly at lower latitudes, makes tropical forestation even more favorable from a climatic perspective by lowering its albedo penalty. Relative to 4C\_SSP3 at 2095, RF<sub>Aer</sub> in 4C\_MF was –71 to –86 mW m $^{-2}$ , and RF<sub>Alb</sub> was 115 to 170 mW m $^{-2}$  (Fig. 3D). The smaller increase in forest cover in 2C\_MF versus 2C\_SSP1 compared with 4C\_MF versus 4C\_SSP3 (Fig. 1) led to smaller RF<sub>Aer</sub>

(–42 to –44 mW m $^{-2}$ ) and RF  $_{\rm Alb}$  (57 to 84 mW m $^{-2}$ ) at 2095 (fig. S6). We note that UKESM1 consistently exhibited higher RF  $_{\rm Alb}$ , highlighting the importance of a multimodel approach.

Changes to organic aerosol can also affect cloud properties, including reflectivity, albeit with the response highly sensitive to background cloud properties (23). Aside from a small region of central Africa, where the radiative impact is much smaller than the forcings from aerosol scattering and surface albedo changes, we found this effect statistically insignificant across almost the entire globe (supplementary materials, Offline Cloud Forcing Calculations) (fig. S7). Although aerosol-driven changes to clouds appear relatively minor, the consideration of aerosol scattering and its partial offsetting of surface albedo-driven warming highlights the greater climatic benefits of tropical forestation and the need to assess the full range of processes by which forestation will affect the Earth system.

# Methane and ozone

The radiative impact of  $\mathrm{CH_4}$  changes ( $\mathrm{RF_{CH4}}$ ) from forestation was generally smaller in magnitude than that of aerosol scattering, and opposite in sign (Fig. 3D). OH was suppressed by reaction with elevated BVOC concentrations in both models, particularly in regions of forest expansion (fig. S8), reducing OH's destruction of  $\mathrm{CH_4}$  (fig. S9) and increasing  $\mathrm{CH_4}$  in both models. We found that forestation at 2095 resulted in a global positive  $\mathrm{RF_{CH4}}$  of 32 to

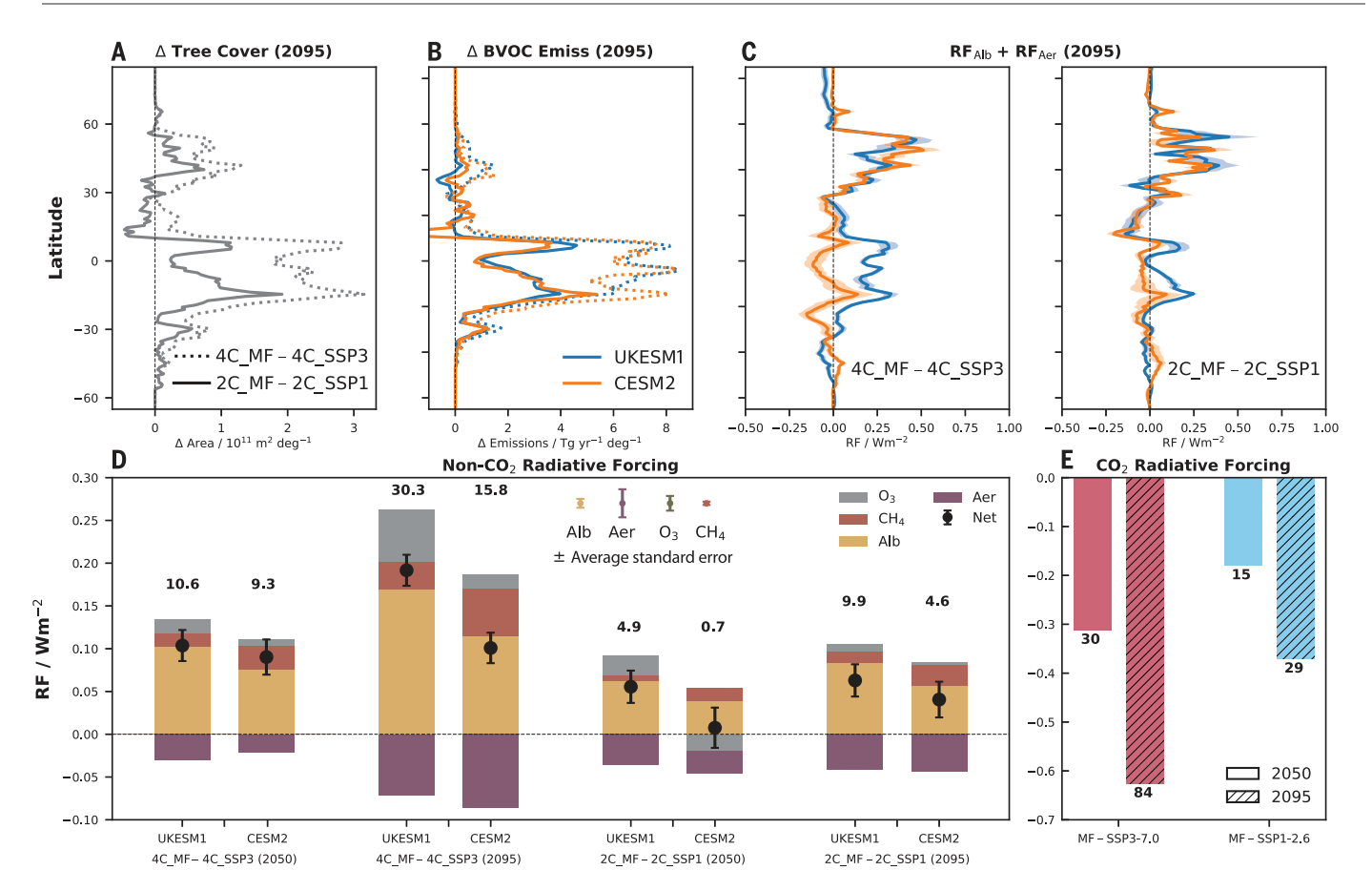


Fig. 3. BVOC emissions, RF<sub>Alb</sub> and RF<sub>Aerr</sub> global mean forcing, and CDR differences. (A, B, and C) Latitudinal changes between 4C\_SSP3 and 4C\_MF (dotted lines) and 2C\_SSP1 and 2C\_MF (solid lines) in (A) tree cover and (B) BVOC emissions and (C) the sum of RF<sub>Alb</sub> and RF<sub>Aer</sub> at 2095 for 4C\_MF and 4C\_SSP3 and 2C\_MF and 2C\_SSP1 at 2095. Shading in (C) represents standard error of the annual zonal mean. In (B) and (C), blue represents data from

UKESM simulations, and orange, from CESM simulation. ( $\mathbf{D}$ ) Global mean of the non-CO<sub>2</sub> radiative forcing (RF<sub>net</sub>) and individual RF components (surface albedo, aerosol scattering, CH<sub>4</sub>, and O<sub>3</sub>) and ( $\mathbf{E}$ ) forcing from CO<sub>2</sub> reduction from additional CDR in Maxforest relative to SSP3-7.0 and SSP1-2.6. Bold values show equivalent change in CO<sub>2</sub> (ppm) (D) and simulated CO<sub>2</sub> change (ppm) (E). Error bars in (D) represent standard error of the mean.

 $57~\rm mW~m^{-2}$  for 4C\_MF relative to 4C\_SSP3, and 12 to 24 mW m $^{-2}$  for 2C\_MF relative to 2C\_SSP1, with CESM2 exhibiting higher RF<sub>CH4</sub> than UKESM1. Notably, the simulation of chemistry in both models featured up-to-date descriptions of the chemistry of isoprene (the most widely emitted BVOC), including important reactions that regenerate OH and thus somewhat buffer its initial depletion (supplementary materials, Earth System Model Simulations).

The response of  $\rm O_3$  to BVOC changes was more complex than that of CH<sub>4</sub>. RF<sub>O3</sub> was positive in all cases except for SSP1-2.6 conditions at 2050 for CESM2 (i.e., 2C\_MF versus 2C\_SSP1), with values of 7 to 20 mW m<sup>-2</sup> (rising to 60 mW m<sup>-2</sup> for 4C\_MF versus 4C\_SSP3 in UKESM1 at 2095), albeit with greater interannual variation than that of RF<sub>CH4</sub> owing to the wide range of factors affecting O<sub>3</sub>. A positive RF<sub>O3</sub> with increasing BVOCs is in qualitative agreement with prior studies (8, 11). The complexity of the O<sub>3</sub> response can be understood

in terms of the strong dependence of net O<sub>3</sub> production on the local chemical environment and the fact that O3 is much more efficient as a greenhouse gas in the upper troposphere than at lower altitudes (24). O<sub>3</sub> can be destroyed by direct reaction with BVOCs, produced in the presence of sufficient NO<sub>x</sub>, and destroyed again under very high NO<sub>x</sub> through titration. This makes the net response highly dependent on regionally variable local conditions, on the pollution scenario (i.e., SSP3-7.0 has higher NO<sub>x</sub> emissions than SSP1-2.6) (fig. S3 and table S1), and, to a lesser extent, on the models, because of differences in their chemical mechanisms. The climatic effect of O<sub>3</sub> is generally comparable to that of CH4 but smaller than the impact of aerosol scattering and surface albedo.

## Carbon dioxide removal

Balancing the positive net RF from albedo and atmospheric composition changes was the additional CDR arising from the forest expansion in Maxforest (figs. S10 to S12). This forestation

led to an average CDR rate of 4.1 to 4.3 billion tonnes of  $\rm CO_2$  per year (GtCO<sub>2</sub> yr<sup>-1</sup>) up to 2050 and 5.0 to 6.5 GtCO<sub>2</sub> yr<sup>-1</sup> up to 2095 (with ranges for 2C and 4C conditions). This is within range of other estimates of biophysical and/or technical CDR potential of afforestation and reforestation of 0.5 to 10.1 GtCO<sub>2</sub> yr<sup>-1</sup> by 2050 (*I*).

By 2095, Maxforest's CDR density (146 and 184 tonnes C per ha (tC ha<sup>-1</sup>) under 2C and 4C conditions, respectively) is also within the range of estimates from other 80-year wide-scale forestation studies, from 72 tC ha<sup>-1</sup> from forestation of dryland regions (7) to ~200 and ~300 tC ha<sup>-1</sup> reported by Bastin *et al.* (21) (deserts, xeric shrublands, and Mediterranean forests) and Griscom *et al.* (25), respectively. The CDR density achieved by forestation was much smaller than that achieved by avoiding deforestation, which was about 500 tC ha<sup>-1</sup> by 2095 in SSP3-7.0. Thus, preventing deforestation is much more efficient than reforestation in terms of mitigation per unit area.

To assess the importance of changes to surface albedo, aerosol scattering, CH<sub>4</sub>, and O<sub>3</sub>, we compared the sum of these components (RF<sub>net</sub>) to the RF that arose from the differences in cumulative CDR (and thus, atmospheric CO<sub>2</sub>) between the Maxforest scenarios and SSP3-7.0 or SSP1-2.6 (RF<sub>CO2</sub>) (supplementary materials, CDR Estimation). Under SSP3-7.0 conditions (4°C warming), the enhanced biosphere carbon sink in Maxforest reduced atmospheric CO<sub>2</sub> by 84 ppm (656 GtCO<sub>2</sub>) relative to SSP3-7.0 by 2095 (32 ppm, 234 GtCO<sub>2</sub> at 2050), causing a negative RF<sub>CO2</sub> (i.e., a cooling) of -660 mW m<sup>-2</sup>  $(-334~\mathrm{mW~m}^{-2}~\mathrm{at}~2050)$  (Fig. 3E). However, the climatic impact of the non-CO<sub>2</sub> changes (RF<sub>net</sub>) associated with the forestation negates  $31 \pm 6\%$ (at 2050) and 23  $\pm$  3% (at 2095) of this reduction (two-model mean with mean uncertainty), indicating that by 2095, Maxforest's forestation has only offset about 14% of SSP3-7.0's projected 420-ppm rise in CO<sub>2</sub>. This finding suggests that using forestation up to the near-biophysical limit is unlikely to reduce CO<sub>2</sub> to levels in line with those of the Paris Agreement's long-term temperature stabilization targets when other climate change mitigation measures are not pursued in tandem.

Under strong climate change mitigation SSP1-2.6 conditions (2°C warming), the additional CDR in Maxforest was lower, with 15 ppm (117 GtCO<sub>2</sub>) at 2050 and 31 ppm (227 GtCO<sub>2</sub>) at 2095 (Fig. 3E and fig. S12) owing to the lower atmospheric CO2 and moderate reforestation in SSP1-2.6 itself (Fig. 1A). However, RF<sub>net</sub> negates less of this additional CDR (18  $\pm$  12% at 2050 and  $14 \pm 5\%$  at 2095; two-model mean with mean uncertainty) than is the case for SSP3-7.0, primarily owing to smaller positive RF from surface albedo and methane changes. By 2095, Maxforest's forestation has offset 50% of the projected 52-ppm rise in CO<sub>2</sub> in SSP1-2.6 from 2015, suggesting that when implemented alongside GHG emission reductions, such forestation could contribute to a future in which end-ofcentury CO<sub>2</sub> levels are close to those of 2015, in contrast to SSP3-7.0.

We note that other mechanisms by which tree cover may affect atmospheric composition, such as fire-related processes (20), ozoneinduced damage (19), and changes in evapotranspiration (26), could influence our study's outcomes. Although the policy of adding trees where they can thrive was central to the Maxforest scenario's development, certain forested areas may be at a higher risk of wildfires. The exact response is uncertain given the range of drivers, including changing temperature and precipitation patterns and population-density growth, a change in vegetation flammability (i.e., flammable grassland replaced by less flammable but longer-burning trees), and potential forestdriven changes to local moisture. Similarly, changes in surface ozone levels have far-reaching implications for carbon uptake, potentially limiting the capacity for  $\mathrm{CO}_2$  removal (19). Moreover, evaporative cooling could be important for surface temperatures in certain regions (27). Our modeling setup is a trade-off that balances climate and Earth system model parameterization uncertainties while minimizing the impact of the complexity of fully coupled interactions.

The changes to atmospheric composition from O<sub>3</sub>, CH<sub>4</sub>, and aerosol scattering, as well as from surface albedo when forest cover was expanded to a near-biophysical maximum, had a net warming effect, which offset up to a third of the  $CO_2$  removal benefit (23 to 31% under SSP3-7.0 conditions and 14 to 18% under SSP1-2.6). However, the negative impact was reduced when forestation occurred alongside reduction of emissions of CO<sub>2</sub> and other pollutants. Our results indicate that for forestation to be an effective climate change mitigation strategy, integration with emissions reduction will be required to avoid driving indirect responses in the Earth system that would diminish its cooling potential.

#### **REFERENCES AND NOTES**

- G.-J. Nabuurs et al., in IPCC, 2022: Climate Change 2022: Mitigation of Climate Change. Contribution of Working Group III to the Sixth Assessment Report of the Intergovernmental Panel on Climate Change, P. R. Shukla et al., Eds. (Cambridge Univ. Press, 2022).
- 2. D. Ellison et al., Glob. Environ. Change **43**, 51–61 (2017).
- N. Seddon, B. Turner, P. Berry, A. Chausson, C. Girardin, Nat. Clim. Chang. 9, 84–87 (2019).
- 4. J. I. Syktus, C. A. McAlpine, Sci. Rep. 6, 29194 (2016).
- International Union for the Conservation of Nature (IUCN), Ecosystem restoration; https://www.iucn.org/our-work/topic/ ecosystem-restoration.
- G. B. Bonan, Science 320, 1444–1449 (2008).
- S. Rohatyn, D. Yakir, E. Rotenberg, Y. Carmel, Science 377, 1436–1439 (2022).
- . G. Thornhill et al., Atmos. Chem. Phys. 21, 1105–1126 (2021).
- 9. J. Weber et al., Nat. Commun. 13, 7202 (2022)
- 10. C. E. Scott et al., Nat. Commun. 9, 157 (2018).
- 11. N. Unger, *Nat. Clim. Chang.* **4**, 907–910 (2014).
- A. Sellar et al., J. Adv. Model. Earth Syst. 11, 4513–4558 (2019).
- G. Danabasoglu et al., J. Adv. Model. Earth Syst. 12, 2 (2020).
- S. Roe, "Terrestrial Systems' Impact on and Response to Climate Change," thesis, University of Virginia (2021). https://10.18130/vpyv-gn70
- 15. K. Riahi et al., Glob. Environ. Change 42, 153–168 (2017).
- P. Forster et al., J. Geophys. Res. Atmos. 121, 12460–12475 (2016).
- A. Guenther et al., Geosci. Model Dev. 5, 1471–1492 (2012).
- J. Weber, J. King, K. Sindelarova, M. Val Martin, Geosci. Model Dev. 16, 3083–3101 (2022).
- S. Sitch, P. M. Cox, W. J. Collins, C. Huntingford, *Nature* 448, 791–794 (2007).
- G. Lasslop, A. Coppola, A. Voulgarakis, C. Yue, S. Veraverbeke, Curr. Clim. Change Rep. 5, 112–123 (2019).
- 21. J.-F. Bastin et al., Science 365, 76-79 (2019)
- 22. R. A. Betts, Nature 408, 187–190 (2000)
- 23. I. Karset et al., Atmos. Chem. Phys. 18, 7669–7690 (2018).
- A. Lacis, D. Wuebbles, J. Logan, J. Geophys. Res. 95, 9971–9981 (1990).
- B. W. Griscom et al., Proc. Natl. Acad. Sci. U.S.A. 114, 11645–11650 (2017).
- 26. L. Boysen et al., Biogeosciences 17, 5615–5638 (2020).
- E. Davin, N. de Noblet-Ducoudré, J. Clim. 23, 97–112 (2009).

- J. Weber, LULC input and CLM5 carbon output "Chemistryalbedo feedbacks offset up to a third of forestation's CO2 removal benefits.", Zenodo (2023); https://zenodo.org/ records/7657286.
- J. Weber, UKESM1 Data accompanying "Chemistry-albedo feedbacks offset up to a third of forestation's CO2 removal benefit", Zenodo (2023); https://zenodo.org/records/7691836.
- J. Weber, CESM2 Data accompanying "Chemistry-albedo feedbacks offset up to a third of forestation's CO2 removal benefits.", Zenodo (2023); https://zenodo.org/records/7692341.
- J. Weber, Soil, litter and vegetation carbon for the 6 simulations performed in CLM5 of "Chemistry-albedo feedbacks offset up to a third of forestation's CO2 removal benef", Zenodo (2023); https://zenodo.org/records/7689779.
- J. Weber, Additional data supporting "Chemistry-albedo feedbacks offset up to a third of forestation's CO2 removal benefits.", Zenodo (2023); https://zenodo.org/records/8338308.
- J. Weber, Plotting code accompanying "Chemistry-albedo feedbacks offset up to a third of forestation's CO2 removal benefits.", Zenodo (2023); https://zenodo.org/records/7851079.

#### **ACKNOWLEDGMENTS**

High-performance computing support from Cheyenne (doi:10.5065/ D6RX99HX) was provided by NCAR's Computational and Information Systems Laboratory, sponsored by the National Science Foundation. This work used Monsoon2, a collaborative high-performance computing facility funded by the Met Office and the Natural Environment Research Council, and JASMIN, the UK collaborative data analysis facility. We thank C. Osborne and D. Edwards for their comments and advice on the manuscript. Funding: This project was funded by the UKRI Future Leaders Fellowship Programme awarded to M.V.M. (MR/T019867/1). Additionally, Y.M.S. was supported by University of Cambridge ESS-DT; C.J.S. acknowledges funding from the NERC/IIASA Collaborative Research Fellowship (NE/T009381/1); and D.J.B acknowledges funding from the Leverhulme Trust (Leverhulme Research Centre grant RC-2015-029). Author contributions: Conceptualization: J.W., J.A.K., M.V.M., D.J.B., and S.R.; Methodology: J.W., J.A.K., M.V.M., N.L.A., Y.M.S., C.J.S., P.L., and S.R.; Investigation: J.W., J.A.K., and D.P.G.; Visualization: J.W., J.A.K., M.V.M., and D.J.B.; Funding acquisition: M.V.M.; Project administration: M.V.M.; Supervision: M.V.M.; Writing - original draft: J.W.; Writing - review and editing: J.W., M.V.M., D.J.B., J.A.K., and S.R. Competing interests: D.J.B. has a minority equity stake in Future Forest/Undo. J.A.K. is on the advisory panel for Ecologi, an organization that invests in ecosystem restoration projects. All other authors declare that they have no competing interests Data and materials availability: Model data from UKESM1, CESM2, and CLM5 are available from the following repositories. All the data are freely available. LULC input data, https://doi.org/10. 5281/zenodo.7657286 (28); UKESM1 data, https://doi.org/10. 5281/zenodo.7691836 (29); CESM2 data, https://doi.org/10.5281/ zenodo.7692341 (30); CLM5 land carbon data, https://doi.org/10. 5281/zenodo.7689779 (31); additional CESM and UKESM data and plotting code, https://doi.org/10.5281/zenodo.8338308 (32); input emissions from SSP3-7.0 and SSP1-2.6 are available from the input4MIPs repository (https://aims2.llnl.gov/) maintained by ESGF; code for making the figures, https://doi.org/10.5281/ zenodo.7851079 (33). The CESM2 code is freely available online and can be downloaded at https://www.cesm.ucar.edu/models. Because of intellectual property right restrictions, we cannot provide either the source code or documentation papers for the Unified Model/UKESM. The Met Office Unified Model/UKESM is available for use under license. For further information on how to apply for a license, see https://www.metoffice.gov.uk/research/ approach/modelling-systems/unified-model. Suite numbers for the runs are listed in the README that accompanies the UKESM1 data repository on Zenodo (29). License information: Copyright © 2024 the authors, some rights reserved; exclusive licensee American Association for the Advancement of Science. No claim to original US government works. https://www.science.org/about/ science-licenses-iournal-article-reuse

# SUPPLEMENTARY MATERIALS

science.org/doi/10.1126/science.adg6196 Materials and Methods Supplementary Text Figs. S1 to S12 Tables S1 and S2 References (34–59)

Submitted 21 April 2023; accepted 15 December 2023 10.1126/science.adg6196